8-2012

Reactions of Methyl Perfluoroalkyl Ethers with Isopropyl Alcohol: Experimental and Theoretical Studies

Howard Knachel
University of Dayton, hknachel1@udayton.edu

Vladimir Benin
University of Dayton, vbenin1@udayton.edu

Chadwick Barklay
University of Dayton, cbarklay1@udayton.edu

Janine C. Birkbeck
B&W Pantex

Billy D. Faubion
B&W Pantex

Part of the *Additional author*

Reactions of Methyl Perfluoroalkyl Ethers with Isopropyl Alcohol: Experimental and Theoretical Studies

Howard C. Knachel* and Vladimir Benin

Department of Chemistry, University of Dayton, Dayton OH 45469

Chadwick D. Barklay

University of Dayton Research Institute, Dayton OH 45469

Janine C. Birkbeck, Billy D. Faubion and William E. Moddeman

B&W Pantex, LLC, Amarillo, TX 79120

- E-mail address: howard.knachel@notes.udayton.edu

Abstract

The reaction of an isomeric mixture of the methyl perfluoroalkyl ether, $C_4F_9OCH_3$ (Novec™-7100), in the presence of isopropyl alcohol (IPA) and/or water has been studied by measuring the rate of product formation using Ion-Selective Electrode (ISE) for fluoride ion, Karl Fisher coulometric titrations for water, and ^1H and ^{19}F NMR spectroscopy for product identification and rate studies. The results showed the methyl perfluoroalkyl ether to be very stable with products forming at the rate of ~1 ppm per year at a laboratory temperature of 20 °C. Measurements over the temperature range of 6 ° to 100 °C were made on samples aged for periods up to 1.8 years.

Density Functional Theory calculations (DFT: *B3LYP/6-31+G(d)*) were employed to investigate different reaction pathways and formulate the probable reaction mechanism. The experimental enthalpy ($\Delta H^{\neq}$) and entropy ($\Delta S^{\neq}$) of activation were determined based on several different kinetic measurements. The $\Delta H^{\neq}$ values are in the range of 20 to 25 kcal/mol and the corresponding $\Delta S^{\neq}$ values range from -32 to -15 cal/mol K. These are in good agreement with the theoretical values. While the range of $\Delta H^{\neq}$ values does not change appreciatively, the $\Delta S^{\neq}$ values are dependent on the proportion of vapor to liquid involved in the reaction of $C_4F_9OCH_3$ with IPA so that the more vapor the more negative the $\Delta S^{\neq}$ value.

Keywords: Novec™-7100, methyl perfluoroalkyl ether, $C_4F_9OCH_3$, DFT, NMR, ion-selective electrode, ISE, enthalpy of activation, entropy of activation, kinetics

Introduction

Substitutes for traditional industrial solvents used to clean surfaces of high-reliability components have been coming on line for several years, due to the Resource Conservation and Recovery Act and the Montreal Protocol on Substances That Deplete the Ozone Layer. Many of these new materials are fluorocarbons, some of which contain organic functional groups. In general, these materials are not ozone depleting, non-carcinogenic, and non-flammable. They are very attractive to potential users, and are being used as pure materials and as the major component in mixtures with certain traditional solvents to increase their cleaning effectiveness.

The focus of this paper is one such material, Novec™-71IPA, a 3M™ Corporation product, referred to as a methyl perfluorobutyl ether-isopropyl alcohol (IPA) azeotrope. It is a mixture of ~ 4.5 wt% IPA in Novec™-7100. The latter is also a 3M™ Corporation product, and it contains three structural isomers of the methyl perfluorobutyl ether, $C_4F_9OCH_3$: (1) $CF_3CF_2CF_2CF_2$-O-CH_3, the normal perfluorobutyl isomer; (2) $(CF_3)_2$-CF-CF_2-O-CH_3, the iso-isomer with a perfluoroisobutyl group; and (3) CF_3CF_2-CF(CF_3)-O-CH_3, the chiral isomer with a secondary perfluorobutyl group. A fourth isomer that has a tertiary perfluorobutyl group is not present. The *n*- and iso-isomers in Novec™-7100 are in about a 40/60 mole ratio, accounting for 99.8 wt% of the mixture.

Early contact with 3M™ Corporation regarding Novec™-71IPA revealed that fluoride ions were found in aged samples by Ion-Selective Electrode (ISE) experiments.[1] The study involved aging samples at a variety of conditions, i.e., temperature, water content, and IPA content. A decision was made by the authors of this paper to determine the source of fluoride ions in aged samples.

A reaction mechanism based on Density Functional Theory (DFT) calculations was proposed. It included the pre-, post-, and transition states (TS), the initial products, and the thermodynamic activation parameters of the rate determining step. The techniques of Karl Fischer titrations for water quantification, ISE for fluoride, and ^{1}H and ^{19}F NMR for identification of products and their rates of formation provided experimental support. Analysis of variance (ANOVA) was applied to the rate data at the 95% confidence level. From this information a rate law was developed. Rate constants measured at several temperatures, allowed the determination of $\Delta H^{\neq}$ and $\Delta S^{\neq}$ which were compared to those predicted by the DFT calculations.

Experimental

Computational Protocol: All calculations were performed using the *Gaussian03/GaussView* software package[2], on a *Linux*-operated *QuantumCube QS16-2500C-X64Q* by Parallel Quantum Solutions.[3] Calculations, unless otherwise specified, were conducted using DFT at the *B3LYP* level with *6-31+G(d)* basis set[4-6], taking into account the fact that for anions, the use of diffuse functions is recommended.[7-10] In several instances, additional calculations were performed at the *MP2/6-31+G(d)* level[11-14], to investigate the role of method on the reactions' kinetic and thermodynamic outcomes. All stationary points were validated by subsequent frequency calculations at the same level of theory. All minimum structures had sets of only positive second derivatives, while TS structures all had one imaginary frequency. In some cases, the relationship of minima and connecting TSs was further verified by Intrinsic Reaction Coordinate calculations.[15, 16] TS searches were conducted employing the Transit-Guided Quasi-Newton method (opt = qst2 or qst3), or the Berny algorithm (opt = TS).[17, 18]

Values of Gibbs free energy and enthalpy changes were obtained after frequency calculations and zero-point energy (ZPE) corrections, which were not scaled. Scaling factors for the ZPE values are available for related levels of theory, such as *B3LYP/6-31G(d)* and *B3LYP/6-31+G(d,p)*, and are 0.9863 and 0.9988 correspondingly, i.e. very close to unity.[19] In addition, since this work was interested in differences of Gibbs free energies (i.e. $\Delta G^{\neq}$ and ΔG values), we anticipated that such values would be largely invariant towards the introduction of the same small correction in the constituent G values. Based on this, we considered scaling ZPE values unnecessary.

The structural parameters derived using the chosen method and level of theory (*B3LYP/6-31+G(d)*) were in excellent agreement with data on the same set of methyl perfluorobutyl ethers, reported in a recent publication.[20] Thus, the calculated bond lengths for the C_{methyl} – O and $C_{perfluorobutyl}$ – O were 1.448 Å and 1.339 Å, compared to 1.436 Å and 1.337 Å, as reported in the literature.[20, 21]

***Chemicals and Materials*:** The Novec™-7100 ether was supplied by the 3M™ Corporation in one gallon glass bottles (H_2O <100 ppm). The IPA was purchased from Sigma-Aldrich (purity >99.5 wt%, H_2O <0.005 wt%, and non-volatile residue <0.0003 wt%).

The need to control the amount of water in many of the experiments necessitated the use of a nitrogen-purged dry box made by Vacuum Atmospheres Corporation, Model HE-43 DRI-LAB. Purified nitrogen was passed through a 40" x 2" column filled with 4Å molecular sieves dried at 400 °C under vacuum. The box also contained open dishes of fresh P_4O_{10} desiccant.

***Preparation of Samples for ISE Fluoride and Water Analyses*:** Sample containers for fluoride ion and water analyses were prepared by modifying 75 mL Pyrex pipettes. The pipettes were cleaned in *aqua regia*, rinsed thoroughly in distilled water and then dried in a 150 °C oven

for several hours. The tip ends of the pipettes were cut back and fire-polished and the top shaft was sealed off to produce a glass tube. The mixtures were created by weighing (on an electronic balance in the dry box) the appropriate amount of Novec™-7100 in the glass tube. The corresponding amount of IPA was added volumetrically using a Hamilton syringe. The open end of the tube was capped with a silicone rubber stopper, the capped tube was removed from the dry box, and the proper amount of H_2O (100, 200 or 500 ppm) was added, also using a Hamilton syringe. The tubes were then connected to a vacuum line**,** cooled in a slurry of dry ice and IPA, evacuated, backfilled with 150 torr of dry O_2 gas to simulate atmospheric conditions, and finally sealed with a torch. A total of 84 tubes were prepared. Thirty of the samples were made with 100 ppm H_2O, 24 samples with 200 ppm H_2O, and 30 samples with 500 ppm H_2O.

The samples were aged in chambers held at 6 °, 26 °, or 46 ° ± 1.0 °C using Cole-Parmer Model 89000 Controllers. Of the 30 tubes with 100 ppm water, 10 samples were aged at 6 °C, 10 samples at 26 °C and the final 10 at 46 °C. Similarly, the other 54 tubes were partitioned and aged in the appropriate chambers. One representative sample for analyses was removed each week from each chamber over a 10 week period.

After removal from the aging chambers, each tube was kept at ≤ -70 °C, to reduce the possibility of additional reactions occurring before analysis. Prior to analysis, the tubes were first warmed to room temperature, returned to the dry box, opened, and the liquid transferred into three pre-dried, 20-mL vials with Teflon gasket screw caps; one vial each for ISE and H_2O analyses plus a backup. The thirty 6 °C samples, having shown no detectable fluoride, were aged again at 36 °C and reanalyzed.

The next batch of 20 samples was prepared such that half contained 2.25 wt% IPA and half contained 9.0 wt% IPA. These samples had < 100 ppm water, were aged at 46 °C and then one tube of each IPA content was analyzed at 1-week intervals for ten weeks.

The final batch of five samples contained 3.5 wt% IPA and was prepared from extra-dry Novec™-7100 and extra-dry IPA. To remove as much water as possible, 4 Å-molecular sieves were dried at 400 °C under vacuum overnight. In the dry box, the sieves were added to capped flasks containing either the Novec™-7100 or IPA. The reagents with the sieves were swirled for more even drying at least once per day for 11 days prior to their mixing and loading in tubes. These five samples were aged at 46 °C with one sample pulled for fluoride and water analyses every two-weeks. ASTM standard procedures were followed to determine water by coulometric Karl Fisher Titration[22] and fluoride by ISE.[23]

Preparation of NMR Samples: Samples for NMR were prepared in the glove box using constricted 5mm Norel S-5-300-8 tubes. Novec™-7100 and IPA were added to the tubes using appropriate Hamilton syringes. The samples were backfilled with dry, 150 torr of O_2 gas to again simulate atmospheric conditions as well as to suppress the longitudinal relaxation time of the nuclei. The tubes were sealed, and their contents analyzed using both ^{1}H and ^{19}F NMR. Longitudinal relaxation times were measured, and the necessary relaxation delays and pulse angles were used to insure that saturation was not a factor in the signal intensity measurements.

Two types of experiments were conducted. In the first, NMR samples were heated in oil baths held at either 78 ° or 90 °C, periodically removed and allowed to cool, analyzed by NMR, and returned to the oil baths to continue aging. Compositions of these samples were 4.5%, 10%, and 15 wt% IPA in Novec™-7100. The hot oil covered the liquid, leaving the top two-thirds of

the tube exposed to ambient temperature. Each sample contained a sealed capillary tube with NMR lock signal and concentration standards.

The second set of NMR experiments involved heating several identically prepared sealed NMR tubes at 80 °, 90 °, or 100 °±1 °C in ovens such that the entire tube was exposed to the same temperature. The refluxing observed in the first set of experiments, was absent in this set. The volume of each sample was 0.300 mL, containing 49 wt% IPA in Novec™-7100. The content of each aged sample was vapor-transferred under vacuum to another NMR tube, containing 0.400 mL of 1.40×10^{-3} M benzene in $CDCl_3$, which was used as a concentration standard for ^1H NMR integrations. Therefore, these samples were not returned to the ovens to continue aging but were single use.

In order to determine the concentration of products in each sample, the total volume of the solution must be known. A Gaertner M911 Cathetometer determined the liquid column height to within 0.05 mm. To calibrate the liquid column height vs. volume relationship, successive additions of 250 μL of liquid were added to an NMR tube using a Hamilton syringe, and the column height was measured. The average calibration value was 18.38 mm per 250 μL.

NMR Instrumentation: Primarily, the ^1H NMR measurements were performed on a Bruker 300 MHz instrument. Fluorine spectra were acquired on a dedicated Anasazi instrument operating at 56.465 MHz.[24] The Anasazi instrument was more suitable for the measurements of neat samples, which yielded very strong NMR signals. Multiscan spectra were recorded using the Batch Averaging capability of the Anasazi PMNR software. A typical spectrum was collected using 2048 batches with two scans per batch. Higher-field instruments were used to examine details of the fine structure and to perform decoupling experiments.

Results and Discussion

***Theoretical Calculations for the Reaction of Perfluoroalkylethers with IPA*:** Several scenarios were investigated involving varying the number of IPA molecules per molecule of methyl perfluoroalkyl ether (Table 1, Cases 1 – 4). Initially, calculations were performed on a truncated system ($CF_3CF_2OCH_3$) using a perfluoroethyl instead of the perfluorobutyl group. Use of the truncated system is based on the assumption that the reaction activation parameters would be largely invariant towards changes in the size of the perfluoroalkyl chain, given the fact that the reaction occurred at the methyl terminus of the system. This assumption was proven correct when subsequent limited calculations on structures with a perfluorobutyl group did indeed show that the chain size had no significant effect on the kinetic and thermodynamic outcome (*vide infra*).

Table 1. Activation parameters for all studied nucleophile-ligand-ether combinations. *Gibbs* free energy and enthalpy differences are in kcal/mol. Entropy differences are in cal/mol K. Results are from *B3LYP/6-31+G(d)* calculations. Italicized results from *MP2/6-31+G(d)* calculations are in parentheses.

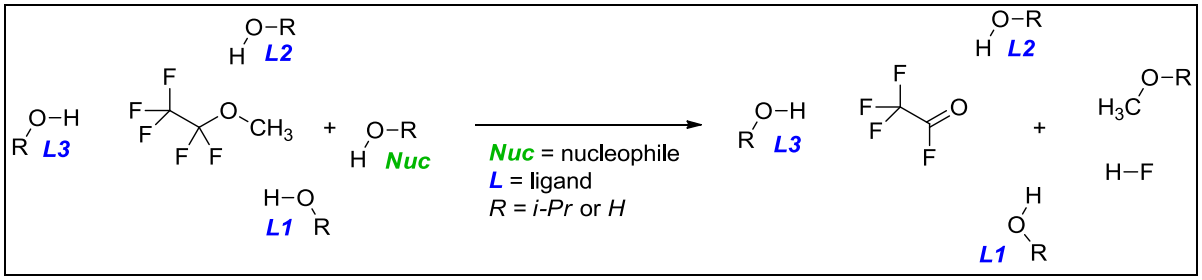

Cases	*Nuc*	*L1*	*L2*	*L3*	$\Delta G^{\neq}$	$\Delta H^{\neq}$	$\Delta S^{\neq}$
1	*i*-PrOH				45.8 *(44.6)*	42.1 *(43.0)*	-12.4 *(-15.5)*
2	*i*-PrOH	*i*-PrOH			36.5 *(36.1)*	31.8 *(32.2)*	-15.9 *(-13.0)*
3	*i*-PrOH	*i*-PrOH	*i*-PrOH		33.4	25.4	-26.8
4	*i*-PrOH	*i*-PrOH	*i*-PrOH	*i*-PrOH	31.4	24.6	-23.0
5	H-OH				55.8	52.3	-11.3
6	H-OH	H-OH			40.8	36.4	-14.7
7	H-OH	H-OH	H-OH		38.3	29.1	-30.9
8	*i*-PrOH	H-OH			36.7	32.0	-15.8
9	H-OH	*i*-PrOH			40.0	35.6	-14.8

10	*i*-PrOH	H-OH	H-OH	32.2	26.5	-19.2
11	H-OH	*i*-PrOH	H-OH	37.5	30.9	-22.0
12	H-OH	H-OH	*i*-PrOH	36.4	28.7	-25.7
13	*i*-PrOH	*i*-PrOH	H-OH	33.2	25.2	-28.2
14	*i*-PrOH	H-OH	*i*-PrOH	33.9	26.9	-23.6
15	H-OH	*i*-PrOH	*i*-PrOH	36.6	28.9	-25.9

The common feature of the first four cases in Table 1 is that, in the gas phase they are concerted processes, leading to the generation in a single step of perfluoro acyl fluoride, hydrogen fluoride (HF) and isopropyl methyl ether (IME). Our efforts to identify potential intermediates, such as the perfluoroethoxy anion or the perfluorinated alcohol, were not successful in either *B3LYP/6-31+G(d)* or *MP2/6-31+G(d)* calculations. All studied reactions reported in Table 1 were moderately exothermic, with the Gibbs free energies in the range of -4.5 to -7.8 kcal/mol.

One of the most important trends evident from Table 1 is related to the dependence of barrier height on the number of alcohol molecules explicitly involved in the reaction. The effect was considerable, particularly upon the change from one to two (***L1***) molecules of IPA, which lead to a reduction of the Gibbs free energy of activation amounting to about 9.0 kcal/mol or 8.5 kcal/mol in MP2 calculations. The barrier was further reduced upon introduction of a third (***L2)*** and again a fourth (***L3***) molecule of IPA, but the change was not nearly as drastic. Clearly the second IPA molecule serves as more than just a solvating agent. As shown graphically in Figure 1, IPA facilitates the formation of HF by serving as both a proton donor to fluorine and a proton acceptor from a second IPA molecule, acting as a nucleophile. The role of this second IPA molecule in HF elimination is similar to the role played by water in previously studied dehydrofluorination reactions of perfluoromethanol and perfluoroethanol.[25-27] In the case of dehydrofluorination, the participation of water as both a proton donor and proton acceptor,

altered the calculated TS geometry from a four- to a six-membered cyclic structure, and drastically lowered the computed activation barrier by at least 15 kcal/mol.

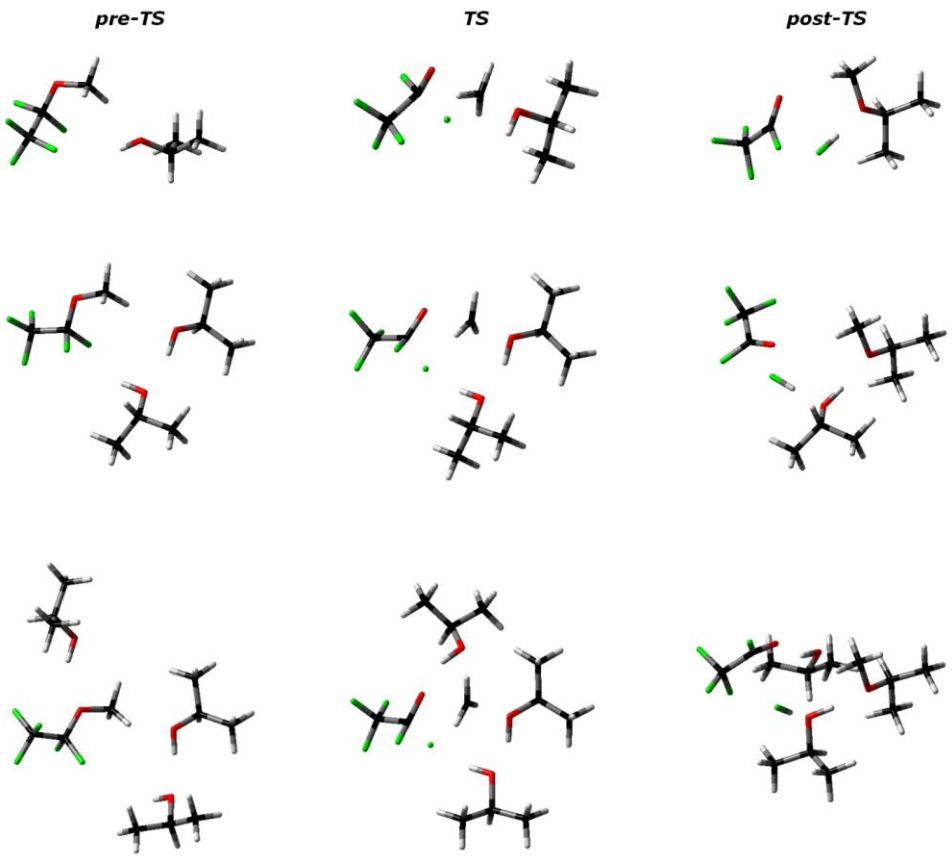

Figure 1. Geometries of all stationary points in the reaction of methyl perfluoroethyl ether with IPA involving one (top), two (middle), or three (bottom) molecules of alcohol. Results are from *B3LYP/6-31+G(d)* calculations.

Sizable negative activation entropy changes were expected in these reactions based on the higher degree of ordering or association of the TS, and they have been confirmed by calculations. It was also noticed that the $\Delta S^{\neq}$ values did not change in equal increments. The changes in $\Delta S^{\neq}$ values were -3.5 cal/mol K (going from one to two IPA molecules), -10.9 cal/mol K (going from two to three IPA molecules) and +3.8 cal/mol K (going from three to four IPA molecules). The changes in $\Delta S^{\neq}$ values are relatively small upon transition from 1 to 2 (or 3 to

4) molecules of IPA, but are more substantial upon transition from 2 to 3 molecules (Table 1). A plausible explanation is suggested, based on the competition between two opposing trends. First, there is an inherent decrease in entropy with an increasing number of IPA molecules, due to the greater ordering of the TS compared to the pre-TS complex. On the other hand, inspection of the relevant geometrical parameters suggests that the TS progressively changes and becomes earlier (and more loose) upon the increase of the number of IPA molecules. Thus, the methyl C to alcohol O distance is increased from 1.69 Å (one molecule IPA) to 1.84 Å (two molecules IPA). This second factor would lead to a TS with a lessening demand for reorganization, thus causing a smaller decrease in entropy. The change in the TS character is most drastic upon transition from one to two molecules of IPA and largely compensates for the introduction of the second IPA molecule. Addition of a third IPA molecule, which serves strictly as a ligand, leads to a substantial negative entropy change because it is more tightly associated in the TS. On the other hand, the fourth molecule's degree of association is almost exactly the same in the pre-TS as it is in the TS, thus leading to a smaller entropy change.

Reaction of Perfluoroalkylethers with Water: In Table 1, Cases 5 – 7 show the results of several calculations involving varying the number of water molecules (from one to three) per molecule of methyl perfluoroalkyl ether. The exhibited trend in reaction barriers is clearly similar to the one observed with IPA. However, for comparable scenarios, the barriers were consistently higher with water. In the case of one molecule of water *vs.* IPA, the difference was about 10 kcal/mol, and with larger numbers of water molecules, the difference was 4 – 5 kcal/mol, leading to the conclusion that for comparable cases, water was consistently the poorer nucleophile. This was further supported by calculations of mixed water/ IPA systems (Table 1,

Cases 8 – 15). In all of these cases, the barriers were consistently higher when water was the nucleophile.

Calculations with the Full-Chain Length Novec™-7100: In order to verify the assumption that using a truncated ether for the theoretical studies was justified, DFT calculations were performed using the Novec™-7100 ether with a perfluorobutyl chain. The calculated enthalpies of activation were, on average, 0.5 kcal/mol lower but the trends remained intact.

The full chain length calculations were also used to investigate reactivity differences between the *n*- and the iso-isomers. The two were found to follow almost iso-energetic pathways, with the branched isomer reacting *via* a slightly lower activation energy barrier, by about 0.5 kcal/mol. The difference is therefore too small for any particular conclusions to be drawn.

Scheme 1

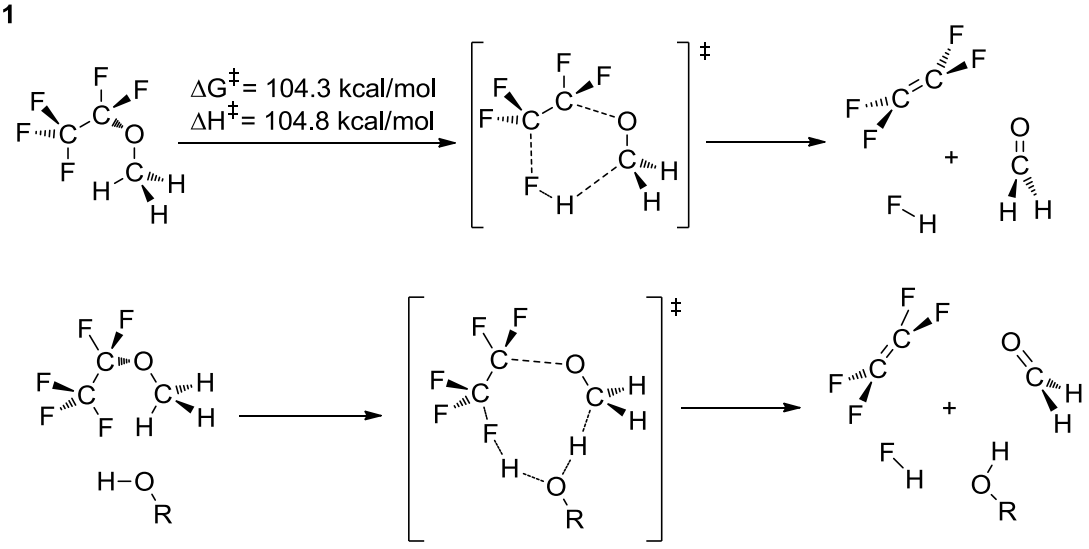

R = H: $\Delta G^{\ddagger}$= 105.4 kcal/mol, $\Delta H^{\ddagger}$= 100.7 kcal/mol

R = *i*-Pr: $\Delta G^{\ddagger}$= 105.4 kcal/mol, $\Delta H^{\ddagger}$= 100.7 kcal/mol

Alternative Mechanisms of Methyl Perfluoroalkyl Ether Decomposition by Dehydrofluorination: The process of intramolecular dehydrofluorination was investigated as an alternative to the nucleophilic substitution reaction. Calculations were done both for the unimolecular and the solvent-assisted processes (i.e. IPA and/or water molecules). The results are summarized in Scheme 1. Based on these much higher activation energies, it is reasonable to assume that dehydrofluorination is not viable for any of the studied systems. The energy gained in HF and H_2CO formation is much less than the energy required for concerted C – F and C – H bond breaking, thus leading to very high activation parameters.

Product Analysis and Kinetics: The particular lot of Novec™-7100 used in this study has 61% of the iso-isomer and 39% of the *n*-isomer. A similar reactivity pattern was observed for the two structural isomers and the results below include concentration measurements on the reaction products from both isomers.

Scheme 2

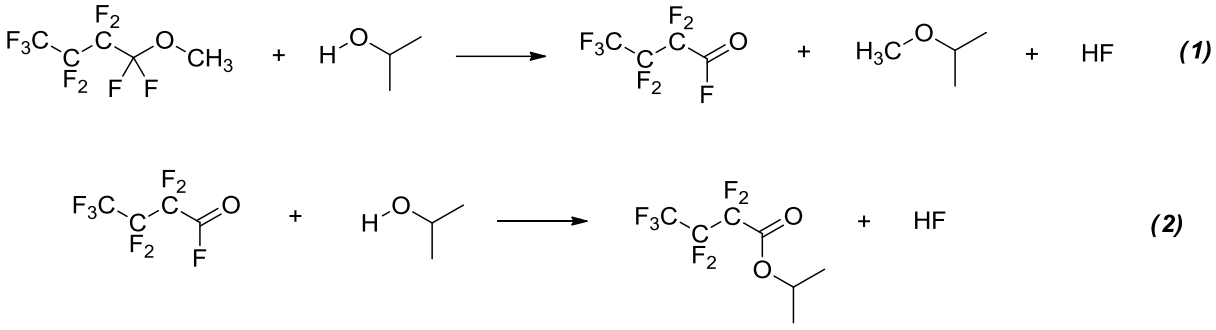

Based on both ^{1}H and ^{19}F NMR results, a reaction pathway has been proposed for the decomposition of the methyl perfluorobutyl ethers in Novec™-7100, and it is represented for the *n*-isomer in Scheme 2. The slower first step (Scheme 2, Equation ***(1)***) leads to the generation of isopropyl methyl ether (IME), HF and perfluoro-*n*-butyryl fluoride, which is supported by the

theoretical results. In the faster second step (Scheme 2, Equation ***(2)***) perfluoro-*n*-butyryl fluoride reacts with IPA to generate the corresponding ester and HF. The same pathway is followed by the iso-isomer of Novec™-7100.

The suggested pathway is supported by the positive identification of the identified products in the reaction mixtures. The first structure is IME, which shows the characteristic signals in the ^{1}H NMR spectrum of a doublet at 1.1 ppm, a singlet at 3.2 ppm and a septet at 3.4 ppm, matching the expected pattern. To obtain definitive proof, IME was prepared independently, according to the Williamson ether synthesis, and then placed in precisely the same solvent mixture. Its ^{1}H NMR spectrum showed a complete match with the studied structure. The second structure, isopropyl perfluoro butyrate, was identified by the signals for the isopropyl group in the ^{1}H NMR spectrum, along with the signals for the perfluoro butyryl moiety in the ^{19}F NMR spectrum. The fluorine signals appear at -81.5, -127.2, and -119.7 ppm for the characteristic triplet, singlet and quartet of the normal ester, respectively. The ^{19}F NMR spectrum for the iso ester has signals at -74.0 ppm (doublet) and -181.7 ppm (septet). Intensity measurements were obtained by integrating the -119.7 ppm and the -181.7 ppm peaks.

The theoretically calculated intermediate structures of perfluoro-*n*-butyryl fluoride and perfluoro-iso-butyryl fluoride were not detected in any of the studies. However, it is a well known fact that acyl fluoride hydrolysis rates, along with acyl halide alcoholosis rates, in general, range between 10^{7} and 10^{12} times faster than rates observed for Equation ***(1)***.[28, 29] Equation ***(2)*** transforms the acyl fluoride into the ester too quickly to be observed by NMR. This fast step produces another molecule of HF in addition to that produced by Equation ***(1)***. In order to use the concentration of fluoride ion to determine the rate of the reaction depicted in Equation ***(1)*** Scheme 2, the total fluoride ion, which is a combination of Equations ***(1)*** and ***(2)***, must be

divided by 2 in order to reflect only that which is produced in Equation ***(1)***. This has implications in the development of the rate law discussed later.

Scheme 3

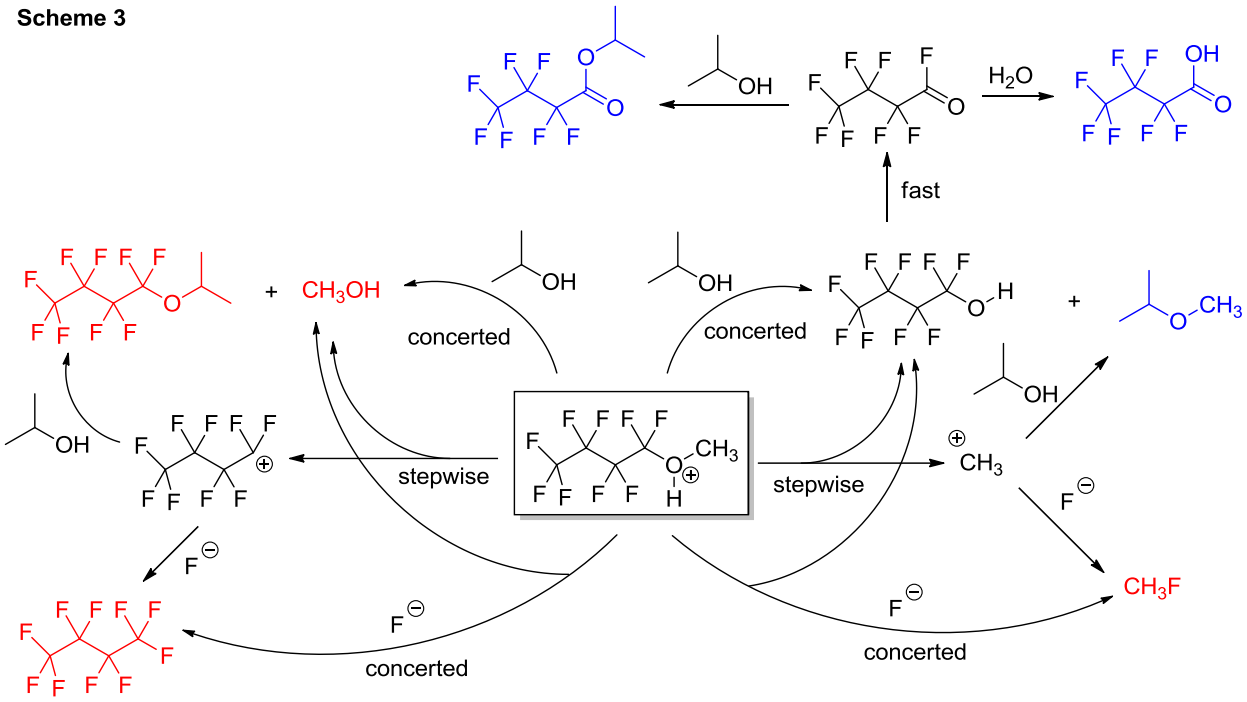

The set of products identified and discussed above can also be formed following an alternative mechanism, which is based on initial protonation of the methyl perfluoroalkyl ether, and is reflected in Scheme 3. Protonation of the starting ether yields the corresponding oxonium ion, which would then deliver a set of products, *via* reactions with available nucleophiles, following either concerted (S_N2) or stepwise (S_N1) pathways. According to Scheme 3, the products discussed above (and highlighted in blue) would still be formed. In particular, the isopropyl perfluorobutyrate and the perfluorobutyric acid would be generated from the intermediate (and short-lived) acid fluoride, which, in its turn, would be generated from perfluorobutanol. The latter, much like other similar perfluoroalcohols, is expected to be very

unstable and quickly decompose. In addition, one would also expect a set of other final structures (highlighted in red). Our careful product analysis has shown, however, that some of these products are not formed, such as methanol or methyl fluoride. The other two, isopropyl perfluorobutyl ether and perfluorobutane cannot be positively ruled out, since their NMR signals appear in the same range as the starting ethers.

In addition to the chemistry outlined in Schemes 2 and 3, another possible route to the formation of perfluoro butyryl fluoride is by the reaction of Novec™-7100 with water, as the nucleophile. Such a reaction would lead to the formation of methanol as one of the products (Scheme 4).

Scheme 4

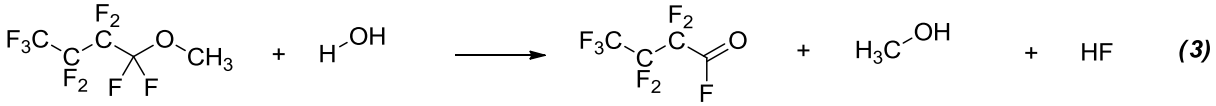

(3)

Methanol however, as mentioned above, has not been identified among the products, eliminating water as a nucleophile. But, water may serve in the capacity of ligand as in Cases 13 and 14 of Table 1, taking the place of IPA. If Case 13 is operative (H_2O as ***L2***), the barrier is almost the same as in Case 3 (IPA as ***L2***). If Case 14 is operative (H_2O as ***L1***), the barrier is higher by 1.5 kcal/mol than in Case 3 (IPA as ***L1***). Therefore water has been included in the rate law expression (Equation 4) for the reaction of Novec™-7100 with IPA, even though it does not serve as the nucleophile. The rate constant at temperature T is k_T, and the reactant concentrations are initial values.

$$Rate_T = k_T * [\text{Novec™-7100}]^a * [\text{IPA}]^b * [H_2O]^c \qquad \text{Equation (4)}$$

***Ion-Specific Electrode Fluoride Data*:** Since ISE is very sensitive to fluoride (~20 ppb detection limit), this technique was used to measure the amount of fluoride produced in samples aged up to 70 days. Fluoride and water analyses were performed on various mixtures of Novec™-7100 with IPA aged at 26°, 36° and 46 °C. Samples aged at 6 °C were also measured by ISE, but the data were not statistically significant and therefore were not included.

Effect of Water: Novec™-7100 and water are immiscible. Water is only present in the Novec™-71IPA because IPA is hygroscopic, making water a minor component of this system. For example, a solution of 4.5 wt% IPA in Novec™-7100 with 100 ppm water is 5.6 M in methyl perfluoroalkyl ether, 1.1 M in IPA, and 8.6×10^{-3} M in water. Since the concentrations of Novec™-7100 and IPA are very large, changes in their values because of interaction with small amounts of H_2O, will not affect their magnitudes. Their values can then be considered as constant. Thus, Equation ***(4)*** can be rewritten as:

$$\text{Rate} = k'_T * [H_2O]^c \qquad \text{Equation (5)}$$

where $k'_T = k_T * [\text{Novec™-7100}]^a * [\text{IPA}]^b$. From Equation ***(5)***, if water influences the rate, one might expect the rate of fluoride formation to change as the concentration of water changes. Therefore, the water concentration was varied to test this hypothesis.

Figure 2 is the plot of the fluoride concentration vs. time at each temperature and water concentration. An Analysis of Variance (ANOVA) was used to analyze the data in Figure 2 at a 95% confidence limit. A calculated p-value that was effectively zero for both temperature and time versus fluoride was found. The analysis showed their direct positive influence on the rate of fluoride production. A p-value of 0.041 for water concentration vs. fluoride showed that the effect of water content, while statistically significant, was not nearly as strong as the relationship

between either fluoride and temperature or fluoride and time. Note that at all three temperatures (26 °, 36 ° and 46 °C) the rate of fluoride production declines as the water content increases. Thus the rate of fluoride formation is weakly dependent on the water concentration and is, in fact, slightly negative (-0.15), i.e., the rate of fluoride production is proportional to $[H_2O]^{-0.15}$.

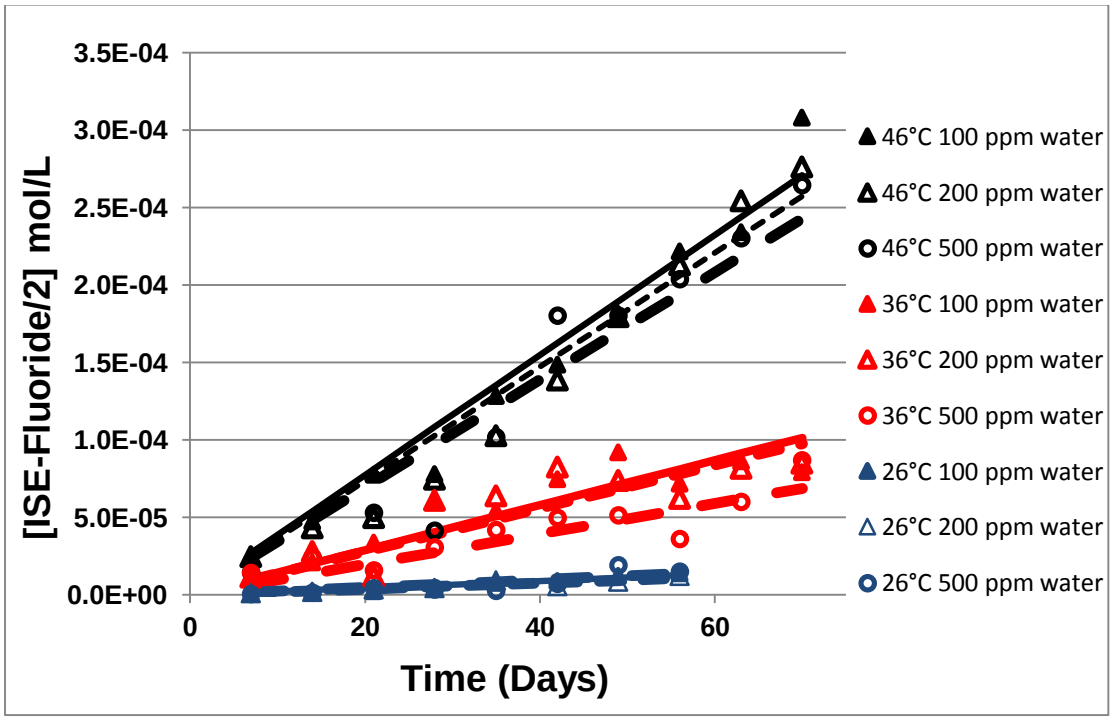

Figure 2. ISE fluoride measurements on Novec™-7100/IPA mixtures aged at three different temperatures (**Blue**, 26 °; **Red**, 36 °; and **Black**, 46 °C) and three different water concentrations (▲▲▲100, △△△200 and ○○○ 500 ppm). Results showed the rate of fluoride produced to increase with increasing temperature and to decrease when H_2O is present at 500 ppm.

From the DFT results (Table 1), when water replaces IPA as ligand ***L1***, as seen when comparing Case 14 with Case 3, the barrier $\Delta H^{\neq}$ increases by 1.5 kcal/mol suggesting that the rate would be slower when water is ***L1*** in place of IPA. In addition, the $\Delta S^{\neq}$ is less negative by 3.2 cal/mol K suggesting decreased organization when water is ***L1***. Water appears to interfere,

by hydrogen bonding with available IPA molecules that are acting as nucleophiles. This is consistent with the inverse relationship for water in the rate law (i.e., c = -0.15).

Effect of IPA: The fluoride data for various IPA concentrations with their water content at 46ºC are plotted in Figure 3 as a function of time. From the slopes of these data, it is clear that the more IPA in Novec™-7100, the faster the fluoride was produced. ANOVA was used to analyze the 46 °C data at a 95% confidence limit. Again, an essentially zero p-value was found, and, in addition, a strong direct influence of time and IPA concentration on fluoride production was observed. Also note that in Figure 3, the plot for 3.5 wt% IPA is not located between the plots of 2.25 and 4.5 wt% IPA, but is actually above the plot for 9.0 wt% IPA. The higher than expected reactivity of the 3.5 wt% IPA samples containing < 1 ppm H_2O can be attributed to their extreme dryness. In fact, the rate of fluoride production of this sample is an order of magnitude larger than otherwise expected. This negative effect between water concentration and fluoride production is consistent with the conclusions from the theoretical study (Table 1) that activation barriers are larger (i.e. reaction rates slower) when water is the ligand (***L1)*** in water-IPA mixtures.

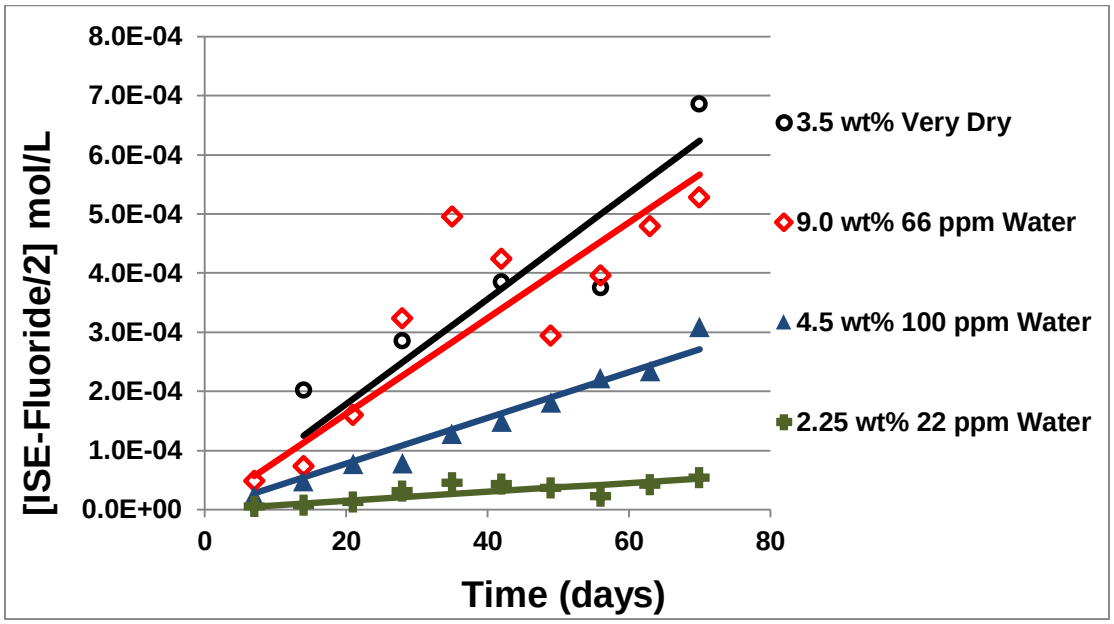

Figure 3. ISE fluoride measurements on Novec™-7100/IPA mixtures aged at 46°C with different IPA concentrations at 2.25 wt% (**Green**), 3.5 wt% (Black), 4.5 wt% (**Blue**) and 9.0 wt% (**Red**). Results showed the rate of fluoride ion produced to increase with increasing IPA, and, in addition, to be the largest for a very dry (< 1 ppm H_2O) mixture, containing 3.5 wt% IPA.

Reaction rates from NMR data: Rate measurements were accomplished by following the growth of the products IME and the isopropyl perfluoro butyrates from the IPA-Novec™-7100 reaction. These products were chosen because they had unique signals, even at low intensities, and their peaks were in regions with minimal interference. In the case of IME, the peaks of the methoxy group at 3.2 ppm in the ^{1}H NMR spectra were integrated. The ^{19}F resonances of the isomeric ester products used for integration are found above in the *Product Analysis and Kinetics* section. These integrals generated the kinetic data, presented in Figure 4, and again confirm the conclusions from the fluoride data, i.e. the reaction products increase with increasing time, temperature and IPA and decreasing water.

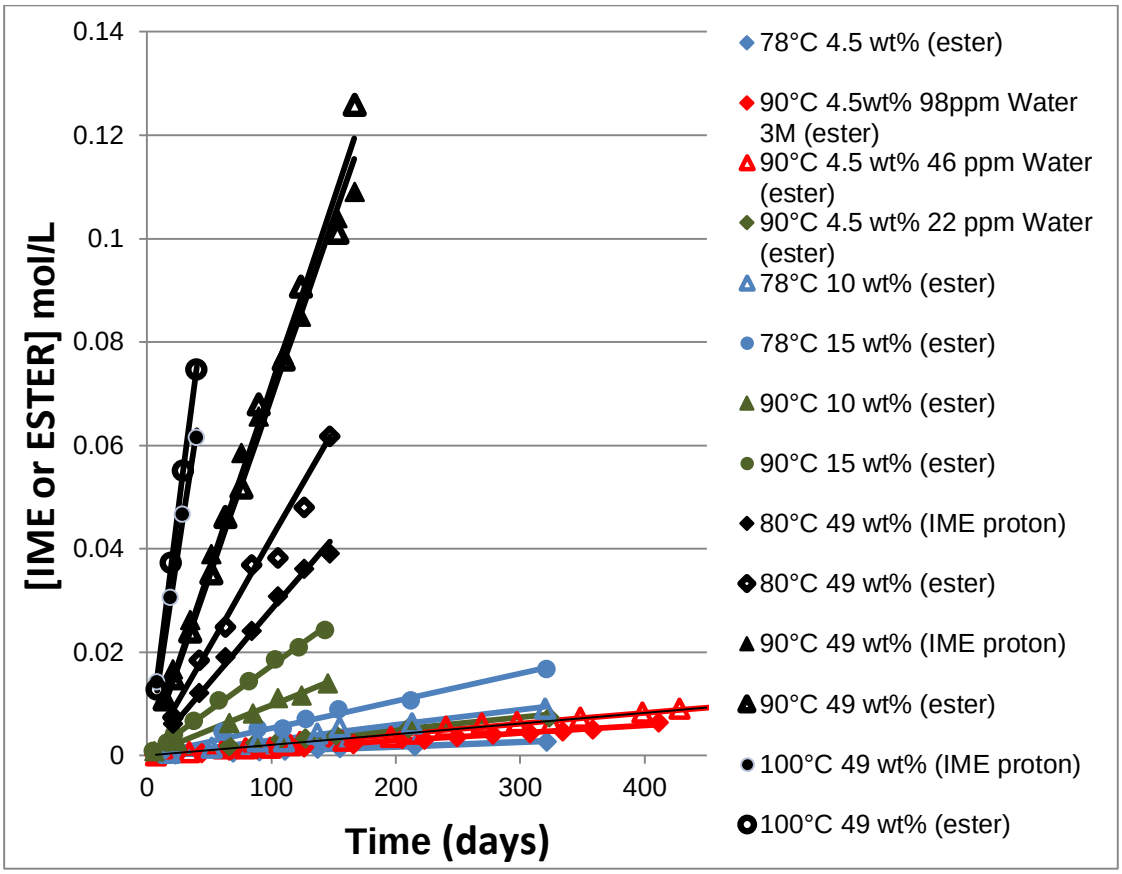

Figure 4. Concentration data based on ^{19}F and ^{1}H NMR signal intensities from Novec™-7100/IPA mixtures aged at 78 °, 80 °, 90 ° or 100 °C, with 4.5, 10, 15 or 49 wt% IPA. [IME] = [Ester] = [Fluoride/2]

Kinetic Model: In order to develop a kinetic model, the low temperature ISE data and the higher temperature NMR data were considered together (Figures 2, 3, and 4). Each of the 25 plots represents an initial rate because of its linearity (average $R^2 = 0.99$). The slope of each line is the reaction rate for that particular sample. To develop the rate law, there are 25 composite rates. However, if one considers each data point on each plot as a rate, there are actually 231 individual rates.

The proposed model was given above in Equation ***(4)***. However, in order to use this model, the exponents of "a", "b" and "c" for the reactants first had to be determined. Typically, the method used to determine the exponents for a reaction involves holding the concentrations of

all but one of the reactants constant and then repeating the experiment as necessary such that each reactant is varied. In the case of these experiments, the value for "c" was already determined to be -0.15, as discussed above. So to determine "b", experiments would normally be conducted where the [Novec™-7100] and [H_2O] are held constant and the [IPA] varied and the reaction rates measured. This would be repeated to determine "a" while holding the [IPA] and [H_2O] constant and varying [Novec™-7100] to measure the reaction rates. Kinetic studies are usually conducted in solvents so it is possible to change the concentration of one reactant while keeping the others constant. However, to avoid interactions between any potential solvent and Novec™-7100 and/or IPA, no solvent was used in this study. Consequently, the concentrations of IPA and Novec™-7100 are not independent of each other. Therefore, the [Novec™-7100] was expressed in terms of the [IPA] by defining N as the ratio of the initial concentration of IPA to that of Novec™-7100. Equation ***(4)*** can now be re-written as Equation ***(6)***.

$$Rate_T = k_T * [IPA]^{a+b} * N^{-a} * [H_2O]^c \qquad \text{Equation } \textbf{\textit{(6)}}$$

To solve for the exponents "a" and "b", all of the measured 231 individual rates appearing in Figures 2 - 4 were used. An ANOVA analysis was applied to these data. The exponents were determined as: "a" = 2.0 and "b" = 2.2. These exponents, along with the previously determined "c", were added to Equation ***(4)*** which is finally rewritten as Equation ***(7)***.

$$\text{Reaction } Rate_T = k_T * [\text{Novec™-7100}]^{2.0} * [IPA]^{2.2} * [H_2O]^{-0.15} \qquad \text{Equation } \textbf{\textit{(7)}}$$

From Equation ***(7)***, the rate constants, k_T for each temperature, were calculated from the appropriate data. Upon closer examination of the rate constants, it became clear that the data fell into three distinct categories. In category 1-ISE, samples were heated in ovens at 26 °, 36 °, and 46 °C. In category 2-NMR, these samples were heated in oil baths at 78 ° and 90 °C, such that two-thirds of each sample tube was not in the oil bath, but rather, was exposed to ambient temperature. Active refluxing was observed during aging, so the exact temperature of the material above the surface of the oil was unknown. Therefore, category 2 samples were not used in determining the rate constants because of the heat loss accompanying condensation on the cooler walls of the container. The samples in category 3-NMR, were heated in ovens at 80 °, 90 °, and 100 °C without exposure to a cooler surface. Samples in categories 1 and 3 were therefore used to determine values of k_T.

The Eyring plot (Figure 5) reveals the $\Delta H^{\neq}$ as determined from the slope of the NMR data to be 20 kcal/mol and the $\Delta H^{\neq}$ as determined from the slope of the ISE-fluoride data to be 25 kcal/mol. When these are compared with the DFT calculations (Table 1), they support the prediction that the process occurs with multiple IPA molecules per molecule of Novec™-7100.

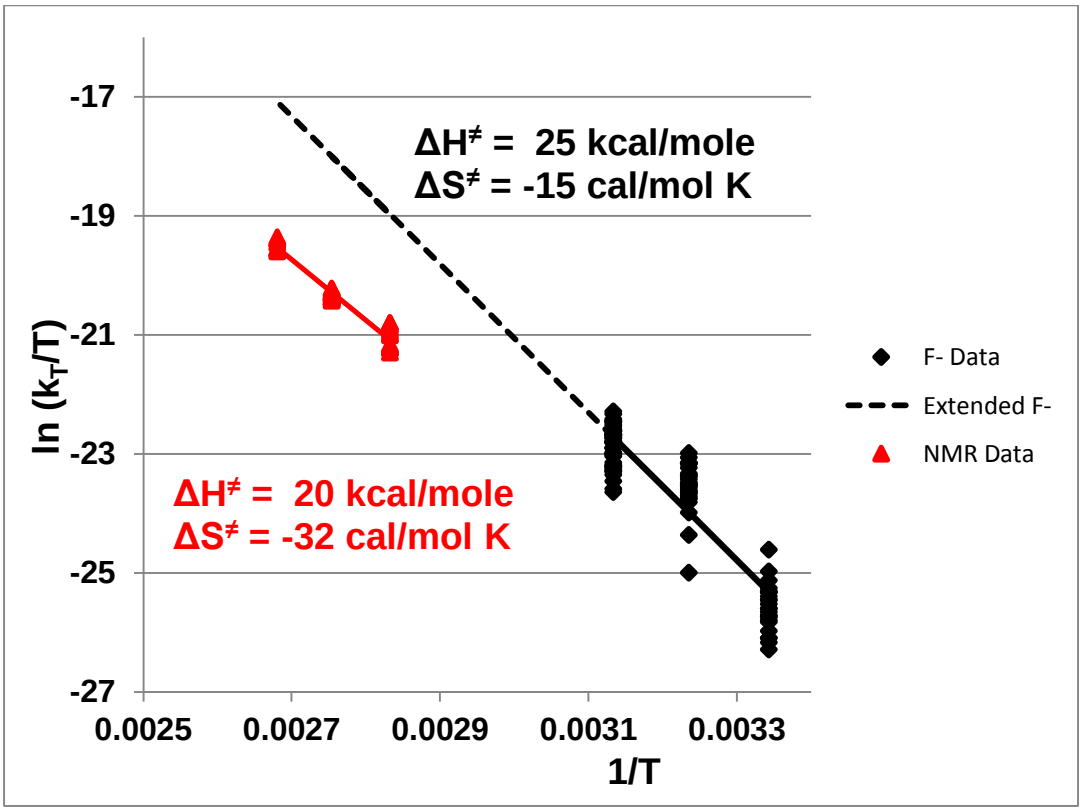

Figure 5. Plot of ln (k_T/T) versus 1/T, which reveals the experimentally determined activation enthalpies ($\Delta H^{\neq}$) and entropies ($\Delta S^{\neq}$).

Basically, there is a very good fit between the $\Delta H^{\neq}$ of the two sets of data (NMR vs. ISE-fluoride). However, there is an observed difference in the results for the activation entropies ($\Delta S^{\neq}$). Both sets yield significant negative entropies of activation, which is consistent with the suggested bimolecular chemistry plus additional ligand molecules. Between the two data sets however, there is a difference of roughly 17 cal/mol K. One plausible explanation that can be advanced is based on the fact that the NMR and ISE-fluoride experiments were conducted in different temperature ranges. While the ISE-fluoride data were collected from samples aged at slightly elevated temperatures, the NMR samples used for the ester/IME analyses were kept at temperatures 50 to 70 °C higher. In the latter case, approximately 20% of each sample was

observed to be in the vapor phase, and therefore a blend of both condensed-phase and vapor-phase reactions would be expected to contribute to the observed reaction rates. Overall, gases possess higher entropy (disorder) compared to the condensed phase. The most favorable TS requires a molecular ratio of 3 or 4 IPA molecules to 1 Novec™-7100 molecule. Such a high degree of organization is unlikely for the gas phase. Note that in Table 1, as the number of IPA molecules in the transition state decreases, the barrier increases leading to a drop in reaction rate as measured by NMR.

Conclusions

This paper explored the aspects of reactions of Novec™-7100 in mixtures with IPA and/or water through a multi-technique approach, utilizing molecular modeling and aging experiments to predict the reaction mechanism and obtain the rates of the chemical reactions under conditions of variable starting material concentrations and temperatures. The analytical techniques used in the rate studies were Ion-Selective Electrode (ISE) for fluoride ion analysis, coulometric Karl Fisher Titration for water analysis, and ^{1}H and ^{19}F NMR spectroscopy to analyze the composition of product mixtures and to follow the growth of particular products. In both sets of experiments, plots of product concentration vs. time were found to be linear (R^2=0.99). The experiments conducted at 46 °C and below, lasted 70 days while the higher temperature experiments were allowed to proceed for time periods exceeding 100 days; the longest being 656 days.

Density functional theory calculations (DFT) were utilized to gain insight on the mechanism for the reactions. Several potential models were explored, but the nucleophilic substitution of the perfluoroalkylether with IPA is the most thermodynamically favorable. This

model suggests concerted methyl transfer and HF elimination, leading to the formation of an acyl fluoride and isopropyl methyl ether (IME). The production of fluoride was confirmed by the ISE analysis while the presence of IME was experimentally confirmed by NMR. The NMR studies could not detect any acyl fluorides, due to their transient nature. NMR experiments also revealed a secondary process whereby the ester, isopropyl perfluorobutyrate, was formed very rapidly from the reaction of the acyl fluoride with IPA.

The DFT calculations provided the thermodynamic activation parameters for the reaction. They also showed the dependence of the activation parameters on the number of IPA molecules involved in the transition state. Only one IPA molecule reacts with the methyl perfluoroalkyl ether, but the presence of 1, 2, or 3 additional IPA molecules in the transition state lowers the activation barrier. The predicted DFT activation energies are in good agreement with those calculated from the experimental rate data for fluoride, esters, and IME accumulation.

The effect of water on the rate of the reaction was determined over the range of < 1 ppm to 500 ppm. According to the rate law derived for the studied reaction, the rate is inversely proportional to the concentration of water, which finds good support in the theoretical studies. Both theoretical studies and experimental results show that water is definitely the poorer nucleophile compared to IPA. Thus, both theoretical and experimental results support the conclusion that 4.5 wt% IPA in Novec™-7100 (Novec™-71IPA), is very stable at ambient temperature producing fluoride at a rate of ~1 ppm/year.

Acknowledgements

This work was supported under the Plant Directed Research and Development Program by the U. S. Department of Energy, National Nuclear Security Administration at the Pantex

Plant, operated by B&W Pantex, LLC under contract number DC-AC54-00AL66620. The authors are grateful to Dr. Tanya Young, Director of Research Support Services at the Department of Chemistry, Ohio State University and Dr. Virginia W. Miner, Acorn NMR, Inc. for many helpful discussions regarding NMR hardware, Nuts software, and interpretation of specialty NMR analyses. Robert W. Ashcraft is gratefully acknowledged for his invaluable statistical guidance. The authors would like to express their appreciation of David A. Hesselroth, Thomas J. Brodbeck, and Jason Kehren of 3M™ Corporation for their candid exchange of information regarding the Novec™ perfluorinated ethers and Thomas A. Kestner also of 3M™ Corporation for sharing his NMR chemical shift assignments with us. Our special thanks to Dr. R. Gerald Keil of the University of Dayton, Department of Chemistry for the many discussions and comments regarding the kinetic measurements.

Supporting Information

Calculated energies and thermodynamic parameters for the stationary points in all studied reactions of methyl perfluoroethyl ether (Tables 1 – 20) and NovecTM7100 (Tables 21 – 22); Experimental rate data from the reactions of methyl perfluoroalkyl ethers with isopropyl alcohol; This material is available free of charge via the internet at http://pubs.acs.org.

References

1. Kehren, J., *Private Communication*, 3M Corporation, Electronics Markets Division, Saint Paul, MN. In.
2. Gaussian 03, R. C., Frisch, M. J.; Trucks, G. W.; Schlegel, H. B.; Scuseria, G. E.; Robb, M. A.; Cheeseman, J. R.; Montgomery, Jr., J. A.; Vreven, T.; Kudin, K. N.; Burant, J. C.; Millam, J. M.; Iyengar, S. S.; Tomasi, J.; Barone, V.; Mennucci, B.; Cossi, M.; Scalmani, G.; Rega, N.; Petersson, G. A.; Nakatsuji, H.; Hada, M.; Ehara, M.; Toyota, K.; Fukuda, R.; Hasegawa, J.; Ishida, M.; Nakajima, T.; Honda, Y.; Kitao, O.; Nakai, H.; Klene, M.; Li, X.; Knox, J. E.; Hratchian, H. P.; Cross, J. B.; Bakken, V.; Adamo, C.; Jaramillo, J.; Gomperts, R.;

Stratmann, R. E.; Yazyev, O.; Austin, A. J.; Cammi, R.; Pomelli, C.; Ochterski, J. W.; Ayala, P. Y.; Morokuma, K.; Voth, G. A.; Salvador, P.; Dannenberg, J. J.; Zakrzewski, V. G.; Dapprich, S.; Daniels, A. D.; Strain, M. C.; Farkas, O.; Malick, D. K.; Rabuck, A. D.; Raghavachari, K.; Foresman, J. B.; Ortiz, J. V.; Cui, Q.; Baboul, A. G.; Clifford, S.; Cioslowski, J.; Stefanov, B. B.; Liu, G.; Liashenko, A.; Piskorz, P.; Komaromi, I.; Martin, R. L.; Fox, D. J.; Keith, T.; Al-Laham, M. A.; Peng, C. Y.; Nanayakkara, A.; Challacombe, M.; Gill, P. M. W.; Johnson, B.; Chen, W.; Wong, M. W.; Gonzalez, C.; and Pople, J. A.; Gaussian, Inc., Wallingford CT, 2004., Gaussian.

3. *Parallel Quantum Solutions*, 2013 Green Acres Road, Suite A, Fayetteville, Arkansas 72703.

4. Becke, A. D., Density-fnnctional Exchange-energy Approximation with Correct Asymptotic Behavior. *Phys. Rev. A* **1988,** 38, 3098 - 3100.

5. Frisch, M. J.; Pople, J. A.; Binkley, J. S., Self-consistent Molecular Orbital Methods 25. Supplementary Functions for Gaussian Basis Sets. *J. Chem. Phys.* **1984,** 80, 3265 - 3269.

6. Lee, C.; Yang, W.; Parr, R. G., Development of the Colle-Salvetti Correlation-energy Formula into a Functional of the Electron Density. *Phys. Rev. B* **1988,** 37, 785 - 789.

7. Chandrasekhar, J.; Andrade, J. G.; Schleyer, P. v. R., Efficient and Accurate Calculation of Anion Proton Affinities. *J. Am. Chem. Soc.* **1981,** 103, 5609 - 5612.

8. Clark, T.; Chandrasekhar, J.; Spitznagel, G. W.; Schleyer, P. v. R., Efficient Diffuse Function-augmented Basis Sets for Anion Calculations. III. The 3-21+G Basis Set for First-row Elements, Li–F. *J. Comp. Chem.* **1983,** 4, (3), 294 - 301.

9. Spitznagel, G. W.; Clark, T.; Chandrasekhar, J.; Schleyer, P. v. R., Stabilization of Methyl Anions by First-Row Substituents. The Superiority of Diffuse Function-Augmented Basis Sets for Anion Calculations. *J. Comp. Chem.* **1982,** 3, (3), 363 - 371.

10. Spitznagel, G. W.; Clark, T.; Schleyer, P. v. R.; Hehre, W. J., An Evaluation of the Performance of Diffuse Function-Augmented Basis Sets for Second Row Elements, Na-Cl. *J. Comp. Chem.* **1987,** 8, (8), 1109 - 1116.

11. Frisch, M. J.; Head-Gordon, M.; Pople, J. A., A direct MP2 Gradient Method. *Chem. Phys. Lett.* **1990,** 166, 275 - 280.

12. Frisch, M. J.; Head-Gordon, M.; Pople, J. A., Semi-Direct Algorithms for the MP2 Energy and Gradient. *Chem. Phys. Lett.* **1990,** 166, 281 - 289.

13. Head-Gordon, M.; Pople, J. A.; Frisch, M. J., MP2 Energy Evaluation by Direct Methods. *Chem. Phys. Lett.* **1988,** 153, 503 - 506.

14. Saebo, S.; Almlof, J., Avoiding the Integral Storage Bottleneck in LCAO Calculations of Electron Correlation. *Chem. Phys. Lett.* **1989,** 154, 83 - 89.

15. Gonzalez, C.; Schlegel, H. B., An Improved Algorithm for Reaction Path Following. *J. Chem. Phys.* **1989,** 90, 2154 - 2161.

16. Gonzalez, C.; Schlegel, H. B., Improved Algorithms for Reaction Path Following: Higher-order Implicit Algorithms. *J. Chem. Phys.* **1991,** 95, 5853 - 5860.

17. Peng, C.; Ayala, P. Y.; Schlegel, H. B.; Frisch, M. J., Using Redundant Internal Coordinates to Optimize Equilibrium Geometries and Transition States. *J. Comp. Chem.* **1996,** 17, 49 - 56.

18. Peng, C.; Schlegel, H. B., Combining Synchronous Transit and Quasi-Newton Methods to Find Transition States. *Israel J. Chem.* **1994,** 33, 449 - 454.

19. Johnson III, R. D.; Irikura, K. K.; Kacker, R. N.; Kessel, R., Scaling Factors and Uncertainties for ab initio Anharmonic Vibrational Frequencies. *J. Chem. Theory Comput.* **2010,** 6, 2822 - 2828.
20. Grubbs II, G. S.; Cooke, S. A., Structure and Barrier to Methyl Group Internal Rotation for $(CF_3)_2CFCF_2OCH_3$ and Its Isomer n-$C_4F_9OCH_3$ (HFE-7100). *J. Phys. Chem. A* **2011,** 115, 1086 - 1091.
21. Grubbs II, G. S.; Cooke, S. A., Conformational Energies of $C_4F_9OC_2H_5$ (HFE-7200). *Chem. Phys. Lett.* **2010,** 495, 182 - 186.
22. ASTM D 6304 "Standard Test Method for Determination of Water in Petroleum Products, L. O., and Additives by Coulometric Karl Fisher Titration".
23. ASTM D 1179 "Standard Test Method for Fluoride Ion in Water".
24. *Anasazi Instruments Inc.*, 4101 Cashard Avenue, Suite 103, Indianapolis, IN.
25. Schneider, W. F.; Wallington, T. J.; Huie, R. E., Energetics and Mechanism of Decomposition of CF_3OH. *J. Phys. Chem.* **1996,** 100, 6097 - 6103.
26. Young, C. J.; Donaldson, D. J., Overtone-Induced Degradation of Perfluorinated Alcohols in the Atmosphere. *J. Phys. Chem. A* **2007,** 111, 13466 - 13471.
27. Takahashi, K.; Kramer, Z. C.; Vaida, V.; Skodje, R. T., Vibrational Overtone Induced Elimination Reactions within Hydrogen-bonded Molecular Clusters: The Dynamics of Water Catalyzed Reactions in CH_2FOH. $(H_2O)n$. *Phys. Chem. Chem. Phys.* **2007,** 9, 3864 - 3871.
28. Bunton, C. A.; Fender, J. H., The Hydrolysis of Acetyl Fluoride. *J. Org. Chem.* **1966,** 31, (7), 2307 - 2312.
29. Hudson, R. F.; Loveday, G. W.; Fiszár, S.; Salvadori, G., Nucleophilic Substitutions in Mixed Solvents. Part III. The Ethanolysis of Acid Chlorides in Solvolytic Media. *J. Chem. Soc. (B)* **1966,** 8, 769 - 774.